27th EPS Conference on Contr. Fusion and Plasma Phys. Budapest, 12-16 June 2000 ECA Vol. **24B** *(2000) 253 -256*

Dynamics of ITB perturbation due to large ELMs in JET

Y. Sarazin [1], P. Beyer [2], C.D. Challis [3], X. Garbet [1], Ph. Ghendrih [1],
E. Joffrin [1], P.J. Lomas [3], V. Parail [3], G. Saibene [4], R. Sartori [4]

[1] *Association Euratom–CEA, CEA Cadarache, F-13108 St-Paul-Lez-Durance, France*
[2] *UMR 6633 PIIM CNRS–Université de Provence, F-13397 Marseille Cedex 20, France*
[3] *Euratom/UKAEA Fusion Association, Culham Science Centre, Abingdon, UK*
[4] *EFDA Close Support Unit, c/o MPI für Plasmaphysik, D-85748 Garching, Germany*

Introduction: Internal Transport Barriers (ITB) are considered as a potentially powerful route toward reactor-relevant plasma scenarios. These barriers, already reported in various tokamaks, are usually found to develop in regions where E×B shear flow and magnetic shear combine to strongly reduce heat (ions and/or electrons) and particle turbulent transport. A correlation with rational q surfaces is also sometimes reported. In JET, such steady Optimised Shear (OS) scenarios with the new MarkII Gas Box divertor exhibit an ELMy H-mode edge. In this case, transitions from small to large amplitude type-III ELMs (Edge Localised Modes), or even to type-I ELMs, are usually associated with a loss of the ITB and a back-transition to a lower confinement state, at constant additional power [1].

This paper documents the propagation of large ELM induced perturbations toward the plasma core, and their interaction with an ITB. Possible physical mechanisms that could account for the observations are also discussed. It is first shown that ELMs generate electron temperature perturbations that propagate on a much smaller time scale than expected from diffusive processes. Recent results from a 3-D turbulent transport model featuring front propagation [2a] are in agreement with the experimental characteristic propagation time of the ELM-induced perturbation [2b]. Then, the induced perturbations are found to penetrate all the deeper since ELM magnitude is large, and may even cross the transport barrier, as also observed numerically [2b]. In that respect, large ELMs are found *(i)* to generate a transient steepening of the ITB, which is followed by *(ii)* an erosion of T_e gradient and *(iii)* an inward movement of the ITB on a diffusive time scale.

Most of the results presented here deal with the pulse #49637, at 2.6T/2.2MA. This is a standard OS discharge with Lower Hybrid pre-heat, that exhibits a core ITB (from about 44.5s) probably located within a region of negative shear [3]. The first large ELM at ~46.41s, occurring during the ramp-down of ICRH (Ion Cyclotron Resonance Heating) power, leads to a drop both in stored energy and in energy confinement time, and a roll-over in the neutron yield. After a recovery phase likely due to the build-up of the edge pedestal during the ELM-free period, confinement and stored energy then degrade continuously after the second huge ELM at ~46.49s, process further amplified by the slow decrease of additional heating.

Part 1 – Propagation of the ELM-induced perturbation: The effect of the ELMs on the core characteristics can be tracked through the ELM-induced electron temperature perturbation δT_e, which may be characterised by:

$$\delta T_e\,(t_n) \;=\; \min_{t_n<t<t_{n+1}}\,[T_e\,(t)] \;-\; T_e\,(t_n - 0.5ms)$$

where t_n corresponds to the time of occurrence of the n^{th} ELM, *i.e.* to the time at which the D_α signal reaches a local maximum. The ELM magnitude is recorded at that specific time. It is worth noting that this may lead to an underestimation of the ELM magnitude if the characteristic growing time of an ELM is much smaller than the diagnostic time step, of order of 100 μs. This may be especially true for small amplitude ELMs. T_e is measured by an ECE radiometer, of 10% absolute accuracy and a noise to signal ratio N/S typically smaller than 3%. Fig.1 shows $-\delta T_e/T_e$ following two large ELMs, together with T_e profiles at the corresponding t_n times. The relative perturbation $\delta T_e/T_e$ may reach 90% at the edge, and appears to strongly decrease at the edge. However, this perturbation remains significant (above 10%) at the ITB location, at around $R = 3.4$m. Furthermore, the ITB does not appear to stop the perturbation propagation, since $\delta T_e/T_e$ does not exhibit any trend of decrease at the very location of the ITB. Further inside the ITB, the perturbation falls below the noise level. The perturbation penetration depth can then be defined as the radius R_{depth} where $\delta T_e/T_e$ falls below typically 8%. It is found that R_{depth} decreases linearly as a function of the ELM magnitude. In particular, ELM magnitudes of order of 3 (a.u.) are sufficient to reach $R = 3.6$m, the typical radius to which expand more conventional ITBs at JET [1]. This puts forward the need to maintain the ELM magnitude below this critical value in ELMy H-mode edge OS scenarios.

The propagation characteristic time of the ELM induced perturbation can be inferred from the cross-correlation $C_x(\tau)$ between D_α and T_e at any ECE channel x (of observation radius R_x): $C_x(\tau) = \langle D_\alpha(t)\ T_{e,x}(t+\tau)\rangle / \langle D_\alpha^2(t)\rangle^{1/2} \langle T_{e,x}^2(t)\rangle^{1/2}$, where $\langle\ldots\rangle$ stands for time average. $C_x(\tau)$ peaks when $|\delta T_e|$ reaches a local maximum, for a positive time lag $\tau_{x,max} = \tau_{burst} + \tau_{relax}$. Here, τ_{burst} is the time taken by the edge cooling, namely the ELM, to propagate up to R_x, while τ_{relax} corresponds to the local relaxation time of the plasma (*i.e.* governed by local transport coefficients). Then, plotting $\tau_{x,max}$ as a function of R_x allows one to determine the effective inward velocity v_{eff} of the perturbation propagation. Large ELM perturbations are found to propagate at $v_{eff} \approx 50$ m/s, which is the order of magnitude of outward-moving avalanche-like events reported on DIII-D [4], possibly suggesting a similar nature of the underlying transport mechanism. Fast acquisition ECE data (250kHz) shown on Fig.2 look very reminiscent of non-local transport experiments [5]. However, no increase in T_e is seen in the core, as sometimes observed in edge cooling experiments. But the large N/S ratio at this high acquisition frequency prevents us to follow the perturbation very deep into the plasma, and more especially to capture the burst propagation across the ITB. Furthermore, T_e decays typically 1.5 10^{-3}s after the ELM event at R_x=3.56m. Assuming the perturbation is initiated at about 3.8m, which is the most outer ECE channel that lies inside the edge pedestal, this gives an estimation of the burst propagation velocity: $v_{burst} \approx 160$ m/s. At least two mechanisms can be invoked to account for such a fast propagation. 1) On the one hand, flux driven turbulence models suggest that turbulent transport consists in avalanche-like events (also called streamers or fronts) characterised by large radial events propagating on time scales consistent with the diamagnetic drift $v^* \sim \rho^* c_s$ ($\rho^* = \rho_s/a$, $c_s^2 = T/m$) [6]. Fronts might be good candidates to explain fast transient events, hardly described by an analysis in terms of convection/diffusion [7]. 2) On the other hand, toroidal coupling allows for a large radial extension of unstable eigenmodes, the so-called global modes [8]. In particular, H-mode edge induced instabilities (such as ELMs) may trigger MHD unstable modes well inside the plasma for large pedestal widths [9]. In this case, the characteristic time scale involves the vertical drift $v_{\nabla B} \sim \varepsilon\, v^*$ ($\varepsilon = a/R$). For shot #49637, this yields $v^* \approx 1500$ m/s and $v_{\nabla B} \approx 500$ m/s, both larger than v_{burst}, making *a priori* difficult any conclusion with respect to the underlying transport mechanism.

At this point, a useful comparison can be however made with recent results obtained with a 3-D resistive ballooning turbulent transport model, featuring avalanche-like events [2a]. A transport barrier can develop when prescribing an external equilibrium shear flow. In this case, when a depression is initiated at the edge, a gradient front is found to propagate inwards with a velocity of order of 170 m/s for typical Tore Supra parameters, smaller than v^* $\approx$ 500 m/s (T=1 keV) and of the same order of magnitude as v_{burst} [2b]. Moreover, the front propagation induced by the depression does cross the transport barrier. These numerical results look in very good agreement with the experimental observations.

Part 2 – ITB perturbation generated by large ELMs: Hereafter, ITB is being characterised by the following set of parameters. Its strength refers to the average of T_e radial gradient length $L_{Te} = -T_e/\partial_r T_e$ over its extension $\Delta_{ITB} = R_2 - R_1$. Here R_1 and R_2 are major radii such that L_{Te} remains larger than $\alpha \times L_{Te}^{min}$ outside the region $[R_1, R_2]$, excluding the H-mode edge barrier (α is an arbitrary coefficient, for which a convenient value has been found to be 3/2). The ITB location radius is then given by $R_{ITB} = (R_2 + R_1)/2$. Fig.3 shows a contour plot of T_e for shot #49637, together with the time evolution of D_α. As mentioned previously, it appears that T_e perturbations induced by large ELMs do cross the ITB, identified with a bold line on this graph. An inward movement of the ITB then appears to be correlated with ELM events. This displacement is consistent with a diffusive time scale, with a characteristic transport coefficient of the barrier of order of $\chi_{ITB} \approx 3.10^{-2}$ m^2/s. It is accompanied by a substantial decay of the ITB strength, of order of 30 %, while additional power only decreases by about 3 % during this period. Also, density increases significantly, likely associated with the build-up of edge pedestal at the start of the ELM-free phase at about 46.25s. Previous transport modelling with the JETTO code suggest that density increase at the edge may trigger both a shrinking of the barrier and an erosion of the gradient [10]. However, Fig.3 shows that this increase by itself is not sufficient in pulse #49637, since these two phenomena clearly appear to be triggered by large ELMs.

Furthermore, it is worth noticing that the erosion of the ITB is not continuous in time. Indeed, Fig.4 shows that ELMs are followed by a transient but significant increase of the gradient at the ITB. This picture is coherent with the paradigm of a front propagation. Whether such an improvement might be sustained if density were to remain constant, or even whether it could lead to the triggering of an ITB itself, still remain speculative but challenging issues. Alternatively, this increase of the gradient might lead to an increase of the turbulent transport and a subsequent erosion of the barrier. Indeed, the short time scale which is involved, shorter than the ion-ion collision time of order of $\tau_{ii} \approx 2.10^{-2}$ s for shot #49637, does not seem to allow for the development of a potentially stabilising radial electric field.

Conclusion: On JET, large ELM induced T_e perturbations are found to propagate inwards on short non-diffusive time scales, consistent with avalanche-like transport models and reminiscent of non-local transport paradigm. This perturbation does cross the ITB for sufficiently large ELMs. Similarly, an edge depression may lead to a front crossing a transport barrier in 3-D avalanche-like transport models. After an ELM, T_e gradient length first increases transiently at the ITB, which then moves inward on a diffusive time scale while degrading. The observations related here allow one to speculate that scenarios exhibiting an ELMy H-mode edge together with an ITB are potentially unstable. Indeed, a substantial reduction of ICRH power seems able to lead to a transition to large ELMs (this transition occurs typically below $P_{ICRH} \approx$ 2MW in pulse #49637). Alternatively, any small degradation of the barrier is likely to generate a substantial heat outflow towards the edge, and thus to trigger a transition to large ELMs. Once large ELMs are triggered, our analysis then shows that ITB is further eroded, leading to a destructive feedback loop. Even though such scenarios have proven achievable at low power [11] or by the mean of impurity injection (such as Argon at JET), they are likely to require an efficient control of the ELM characteristics when going to reactor relevant developments [12].

Acknowledgements: The authors are pleased to thank J.M. Chareau for his help in validating T_e ECE data. This work was done partly in the framework of the JET Joint Undertaking.

References: [1] F.X. Söldner et al., *Plasma Phys. Controlled Fusion* **39** (1997) B353.
[2] (a) P. Beyer, S. Benkadda, X. Garbet, P.H. Diamond, *submitted to Phys. Rev. Let.;* (b) P. Beyer, *private communication.* [3] C.D. Challis et al., *contributed oral paper, this conference.*
[4] P.A. Politzer, *Phys. Rev. Let.* **84** (2000) 1192.
[5] J.D. Callen & M.W. Kissick., *Plasma Phys. Controlled Fusion* **39** (1997) B173.
[6] B.A. Carreras et al., *Phys. of Plasmas* **3** (1996) 2902; X. Garbet et al., *Nuc. Fusion* **11Y** (1999) 2063.
[7] Y. Sarazin, X. Garbet, Ph. Ghendrih, S. Benkadda, *Phys. of Plasmas* **7** (2000) 1085.
[8] J.W. Connor et al., *Phys. Rev. Let.* **70** (1993) 1803; F. Romanelli, F. Zonca, *Phys. Fluids B* **5** (1993) 4081.
[9] L.L. Lao, *Plasma Phys. Controlled Fusion* **42** (2000) A51.
[10] V. Parail, *private communication.* [11] O. Gruber et al., *Phys. Rev. Let.* **83** (1999) 1787.
[12] M.F.F. Nave et al., *this conference*; R. Sartori et al., *this conference*.

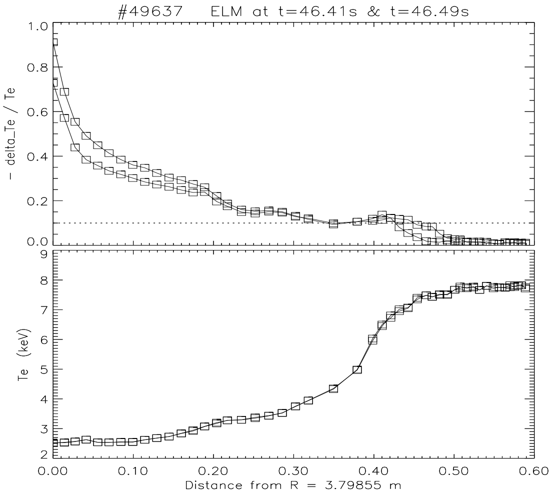

Figure 1: *T_e perturbation (a) and T_e profile (b) vs distance from most outer ECE channel.*

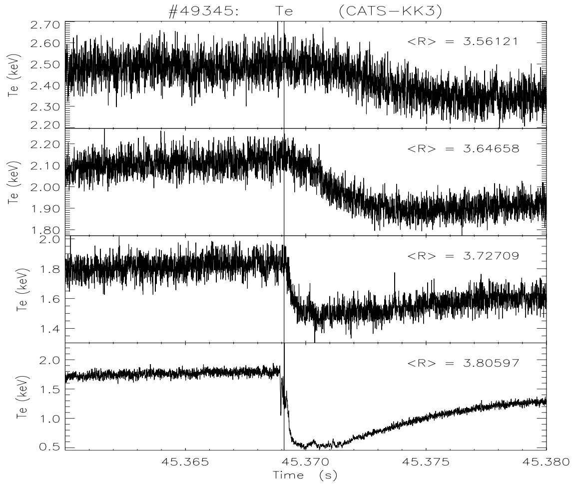

Figure 2: *T_e at various radii (ECE). The vertical line refers to an ELM event.*

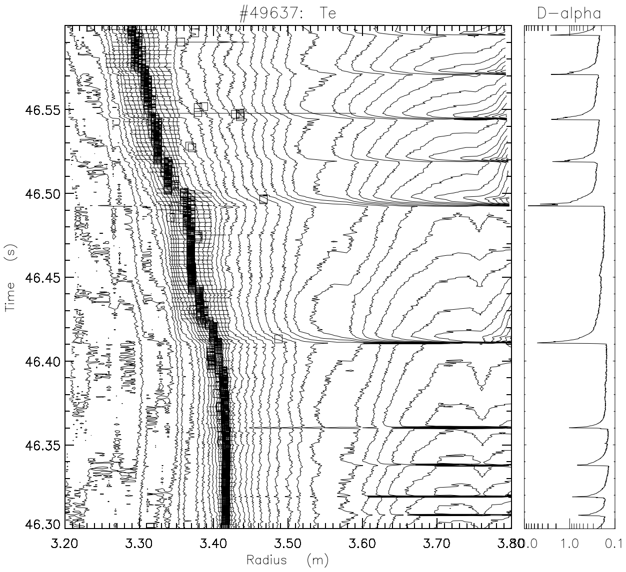

Figure 3: *Contour plot of T_e, R_{ITB} (bold), Δ_{ITB} (horiz. lines), and D_α signal (a.u.).*

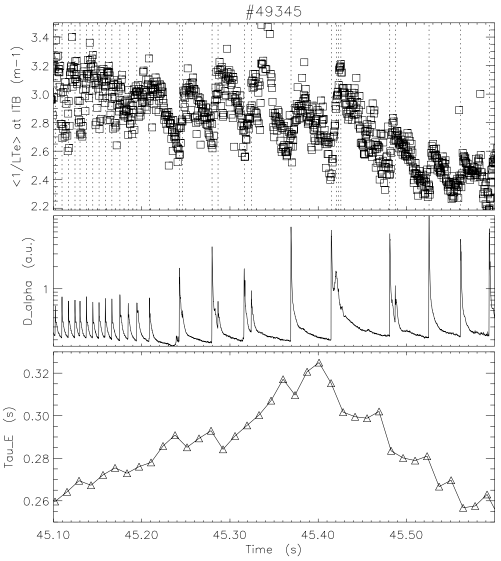

Figure 4: *ITB strength, D_α signal and τ_E. Dashed lines refer to ELM events.*